Self-Assembled Cationic Nanoparticles Combined with Curcumin against Multidrug-Resistant Bacteria

Jian Bin Zhen,*,|| Jiajia Yi,|| Huan Huan Ding, and Ke-Wu Yang*
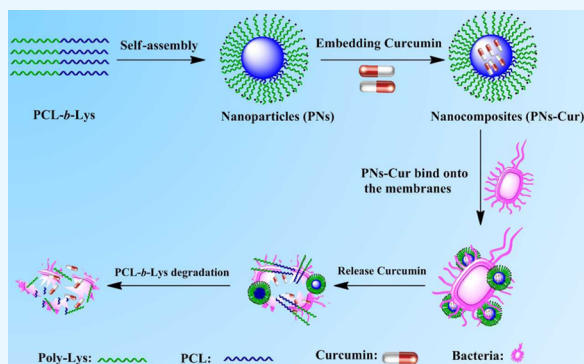
ACCESS | Metrics & More | Article Recommendations | Supporting Information

ABSTRACT: The overuse of antibiotics exacerbates the development of antibiotic-resistant bacteria, threatening global public health, while most traditional antibiotics act on specific targets and sterilize through chemical modes. Therefore, it is a desperate need to design novel therapeutics or extraordinary strategies to overcome resistant bacteria. Herein, we report a positively charged nanocomposite PNs-Cur with a hydrodynamic diameter of 289.6 nm, which was fabricated by ring-opening polymerization of ε-caprolactone and Z-Lys-N-carboxyanhydrides (NCAs), and then natural curcumin was loaded onto the PCL core of PNs with a nanostructure through self-assembly, identified through UV−vis, and characterized by scanning electron microscopy (SEM) and dynamic light scattering (DLS). Especially, the self-assembly dynamics of PNs was simulated through molecular modeling to confirm the formation of a core−shell nanostructure. Biological assays revealed that PNs-Cur possessed broad-spectrum and efficient antibacterial activities against both Gram-positive and Gram-negative bacteria, including drug-resistant clinical bacteria and fungus, with MIC values in the range of 8−32 μg/mL. Also, in vivo evaluation showed that PNs-Cur exhibited strong antibacterial activities in infected mice. Importantly, the nanocomposite did not indeed induce the emergence of drug-resistant bacterial strains even after 21 passages, especially showing low toxicity regardless of in vivo or in vitro. The study of the antibacterial mechanism indicated that PNs-Cur could indeed destruct membrane potential, change the membrane potential, and cause the leakage of the cytoplasm. Concurrently, the released curcumin further plays a bactericidal role, eventually leading to bacterial irreversible apoptosis. This unique bacterial mode that PNs-Cur possesses may be the reason why it is not easy to make the bacteria susceptible to easily produce drug resistance. Overall, the constructed PNs-Cur is a promising antibacterial material, which provides a novel strategy to develop efficient antibacterial materials and combat increasingly prevalent bacterial infections.

INTRODUCTION

Antibiotics have played an important role in treating a wide range of Gram-positive and Gram-negative bacterial infections over the past 70 years.[1−3] However, the overuse of antibiotics has resulted in more and more drug-resistant bacteria, posing a great threat to public health.[4−8] According to the report from the World Health Organization (WHO),[9] the rapid development of antibiotic-resistant pathogens has been listed as one of the greatest threats to global health; generally, traditional antibiotics, such as ciprofloxacin, doxycycline, and ceftazidime, sterilize in chemical ways but cannot physically destroy the membranes of the bacteria,[10,11] and consequently, the morphology of bacteria is preserved, giving bacteria the opportunity to develop drug resistance and exacerbating the emergence of bacterial drug resistance.[11−13] To this end, it is urgently needed to explore new types of therapeutics and antibacterial agents that act in different ways from those of commercially small-molecule antibiotics.[14,15]

Toward this goal, a large number of macromolecular antibacterial materials, such as quaternary ammonium moieties, carbon-based nanomaterials, antibacterial peptides, and N-halamine polymers, have been widely studied.[13,16−21] These materials carry enriched antibacterial groups and have better selectivity toward bacteria than mammalian cells.[22] Especially, cationic polymers with amphiphilic structures have attracted wide attention as the most promising substitutes for antibiotics because they have excellent activities[23] and rapid onset of killing and are less prone to develop drug resistance, and so on.[24−26] Amphiphilic cationic polymers can bind to bacterial membranes via electrostatic interactions, prompting the hydrophobic groups in polymers to penetrate into the lipophilic domain of the membranes and then tear the membranes, eventually leading to the leakage of intracellular contents and lysis of bacterial cells.[27−29] The unmatched

Scheme 1. Synthetic Route of PCL-NH₂

Z: PCL-NH-Z PCL-NH₂
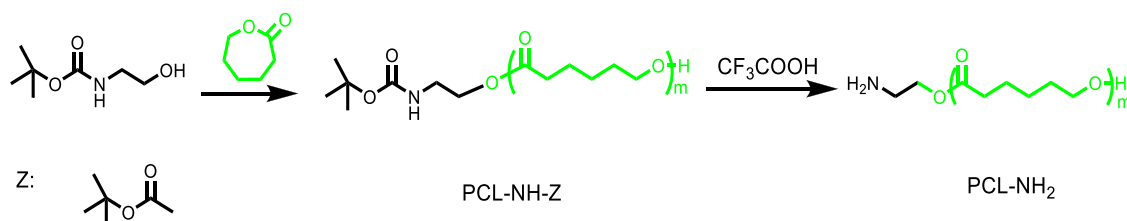
Scheme 2. Synthetic Route of PCL-*b*-Lys

Cbz:
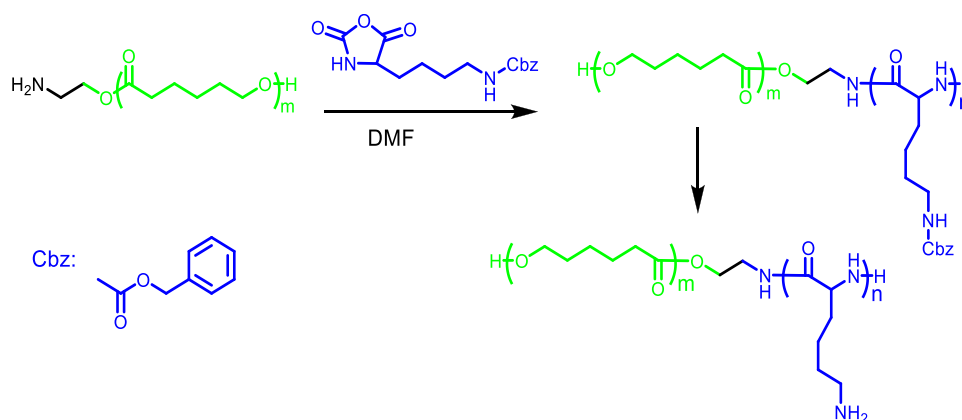
sterilization mode makes it difficult for bacteria to develop drug resistance.[30] In addition, with the rapid development of nanotechnology in the past few decades, antibacterial nanomaterials have also attracted great attention recently because of their unique properties such as ultra-small size and good biocompatibility.[13,19,31−34]

Amphiphilic polymers composed of hydrophilic and hydrophobic sections could self-assemble into nanoparticles with core−shell structures,[29,35−38] which can improve the antibacterial activities and biocompatibility of the polymers. The nanoparticles with a high concentration of positive charge can quickly and tightly adhere to the cell surface,[39−41] followed by the physically forced penetration of hydrophobic groups into the bacterial wall,[42] ultimately resulting in the irreversible apoptosis of the bacterial cells.[43,44] Importantly, these types of polymers do not easily induce the pathogens susceptible to engender drug resistance.[43−45] Moreover, curcumin, a natural polyphenolic compound, could be extracted from the rhizomes of the herb Curcuma longa.[46,47] It is a highly potent nontoxic and cheaper drug that possesses a wide range of biological activities, such as antibacterial, anti-inflammatory, and anticancer properties.[47,48] However, the aqueous solubility of curcumin is poor, which greatly limits its applications in clinics.[49,50] Moreover, for some difficult and miscellaneous infections, monotherapy is clearly inadequate, and physicians usually require combination therapy of multiple drugs to achieve therapeutic purposes. Therefore, it is a wonderful idea to design decent nanocarriers with antibacterial activities, which can not only overcome the solubility of curcumin but also exert synergistic antibacterial effects.[51,52]

In this study, we reported a facile, low-cost, and effective combination therapy for defeating complicated drug-bacterial infections. First, we constructed an amphiphilic cationic polymer composed of polycaprolactone (PCL) and polylysine (PLys) chains, which can self-assemble into nanoparticles (PNs) with the structure of a hydrophobic PCL core and a positively charged PLys shell,[53] Then, the biodegradable nanoparticles with antibacterial properties, acting as the nanocarrier, incorporated curcumin into the core of PNs. In this approach, the positively charged PNs possessed great cytocompatibility and low toxicity toward mammalian cells, which acting as a "nanomissile," could directly bind onto the bacterial membranes by nonspecific electrostatic interaction[54] and then pierce into the phospholipid layer of cell membranes. Simultaneously, the curcumin embedded in the nanoparticles could be gradually released once interacting with the bacterial membranes, which is due to the degradation of PCL and PLys chains.[55] We found that the nanoparticles carrying curcumin exhibited excellent antimicrobial effects without any detectable toxicity to mammalian cells and especially drug resistance. In addition, the designed nanoparticles (PNs) as a carrier also could be decorated with traditional antibiotics or other insoluble drugs.

■ RESULTS AND DISCUSSION

Synthesis and Characterization of PCL-*b*-Lys. Inspired by our previous work, the amphiphilic polymer PCL₁₆-*b*-Lys₁₆ (PCL-*b*-Lys) was synthesized via ring-opening polymerization of monomers ε-caprolactone and Z-Lys-NCAs and the deprotection process. Subsequently, the prepared polymer self-assembled into nanoparticles. Considering various factors, including self-assembly, bactericidal ability, and biocompatibility, PCL-*b*-Lys with a ratio of 1:1 of hydrophilic to hydrophobic monomers was constructed. The synthetic route of the PCL-*b*-Lys copolymer is shown in Schemes 1 and 2. First, the NCA monomer Cbz-Lys-NAC was synthesized by the cyclization reaction of Lys-Cbz with triphosgene as our previous work. Under methanesulfonic acid (MSA) catalysis, the initiator N-Boc-ethanolamine initiated the polymerization of the monomer ε-caprolactone via ring-opening reaction. After the reaction mixture was precipitated in methanol, the

intermediate product (PCL-NH-Z) was deprotected to give the polymer PCL-NH$_2$.

The structure of PCL-NH$_2$ was characterized by ^{1}H NMR (Figure S1). As shown in Figure S1, the degree of polymerization (DP) of PCL in the polymer PCL-NH$_2$ was calculated to be 16 by comparing the integral area of peak f (methylene, $-CH_2-NH_2$) and peak a (methylene, HO$-$CH$_2-$, in PCL chains). Then, PCL-NH$_2$, as a macroinitiator, initiated the ring-opening polymerization of Cbz-Lys-NCA in anhydrous DMF to offer the polymer PCL-*b*-Lys-Cbz. As shown in Figure S2, the chemical structure of PCL-*b*-Lys-Cbz was demonstrated by the ^{1}H NMR spectrum. The DP of Lys-Cbz in PCL-*b*-Lys-Cbz was calculated to be 16 by comparing the integral area of peak a (methylene, HO$-$CH$_2-$) and peak k (methylene, in the Ph$-$CH$_2-$OCO$-$). The deprotection of the poly-Cbz-lysine block offered the target amphiphilic linear polymer PCL-*b*-Lys, which was verified by ^{1}H NMR. As shown in Figure S3, the peaks corresponded to the protons of PCL-*b*-Lys, and the DP of the Lys monomer in PCL-*b*-Lys was verified to be 16, indicating the successful fabrication of the amphiphilic copolymer PCL-*b*-Lys. Meanwhile, it is worth noting that the critical nanoparticle concentration (CNC) of amphiphilic PCL-*b*-Lys is 11.22 μg/mL (Figure 1). In addition,
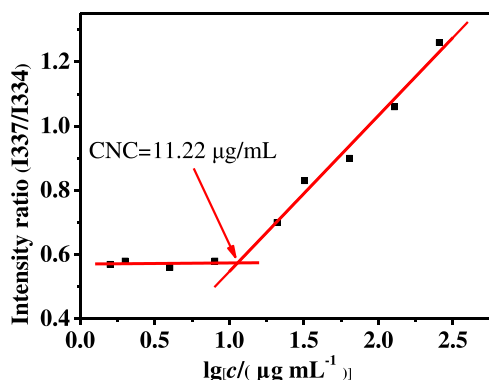

Figure 1. Determination of the critical nanoparticle concentration of PNs (PCL-*b*-Lys).

as shown in Figure S5, the molecular weight measured by GPC (Mw = 6488) is lower than that measured by NMR due to different mechanisms. The low PDI (1.04) indicates the controlled polymerization. According to GPC, the degree of polymerization (PD) of PCL-*b*-Lys was 15, which was similar to the result of NMR.

Preparation and Characterization of the Nanocomposite PNs-Cur. Amphiphilic PCL-*b*-Lys (PNs) could self-assemble into nanoparticles, enabling a more efficient and strong interaction with bacterial cells. With the degradation of nanoparticles, the released curcumin would further exhibit antibacterial efficacy. A nanocomposite (PNs-Cur) composed of PCL-*b*-Lys and curcumin was fabricated according to the following steps. First, amphiphilic PCL-*b*-Lys self-assembled into nanoparticles (PNs) with hydrophobic PCL cores and hydrophilic PLys shells in aqueous solution. Especially, the positively charged nanocomposite PNs-Cur (+28.6 mV) could maintain long-term stability for a few months due to the bare amino groups ($-NH_2$) of the PLys block. The successful fabrication of the nanocomposite PNs-Cur was verified by UV$-$vis. As shown in Figure 2, the individual PNs had no obvious absorbance at the wavelength range of detection, but
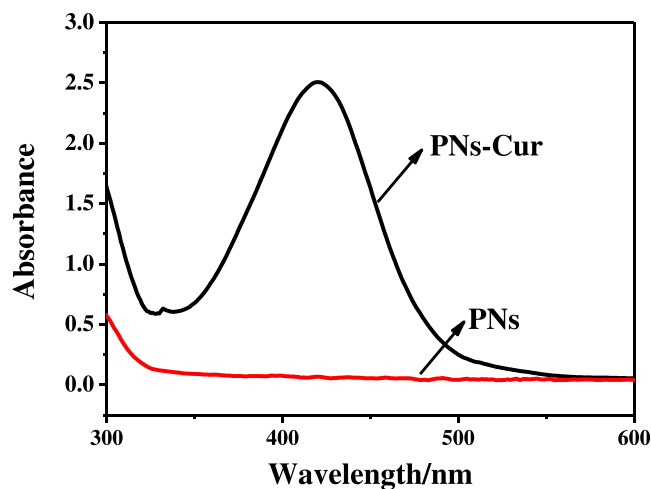

Figure 2. UV$-$vis spectrogram of PNs-Cur.

the nanocomposite showed a maximum absorption peak at 425 nm, indicating that curcumin was encapsulated into the hydrophobic core of PNs.

The self-assembly dynamics of PCL-*b*-Lys (PNs) was simulated through molecular modeling using Material Studio 5.5 software. As shown in Figures 4C and S7, the amphiphilic polymer could indeed self-assemble into core$-$shell-structured nanoparticles consisting of a hydrophobic core of PCL and a hydrophilic shell of Lys$_{16}$. In addition, the hydrodynamic diameter of the nanocomposite (PNs-Cur) was determined by dynamic light scattering (DLS) to be 289.6 nm with a narrow polydispersity index (PDI) of 0.26 (Figure 3A). After the amphiphilic copolymer PCL-*b*-Lys self-assembled into nanoparticles (named PNs) in THF/H$_2$O, a drop of the nanoparticles was spread on the silicon wafer and freeze-dried. Samples were treated with gold before observation. The results showed that the morphology of PNs-Cur was spherical nanostructures with a diameter of around 220 nm (Figure 3B), which is reasonably smaller than the size determined by DLS. Meantime, we also observed the size and morphology of PNs by DLS and SEM. As shown in Figure 4A,B, the hydrodynamic diameter of PNs was 218.5 nm and the polydispersity index (PDI) was 0.15 (Figure 4A), of which the morphology was spherical with a diameter of around 200 nm (Figure 4B).

Curcumin Release Analysis. The loaded curcumin was confirmed due to the absorbance peak at 425 nm through UV$-$vis characterization. The amount of curcumin was measured based on the established calibration curve (Figure S4), by which we can calculate the drug loading efficiency (DLE) and the drug loading content (DLC) as follows

$$DLC(\%) = \frac{\text{weight of drug encapsulated in nanoparticles}}{\text{weight of polymer}}$$
$$\times 100\%$$
$$= 6.5\%$$

$$DLE(\%) = \frac{\text{weight of drug encapsulated in nanoparticles}}{\text{weight of drug in feed}}$$
$$\times 100\%$$
$$= 25.6\%$$

Lipase-Triggered Curcumin Release Study in Vitro. Generally, lipases, existing in different strains, could easily
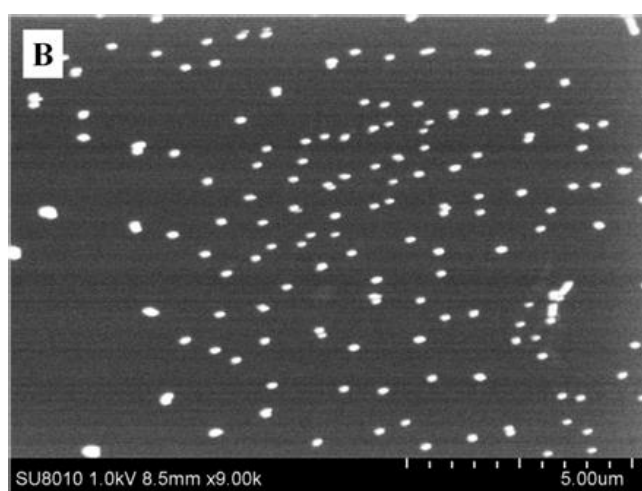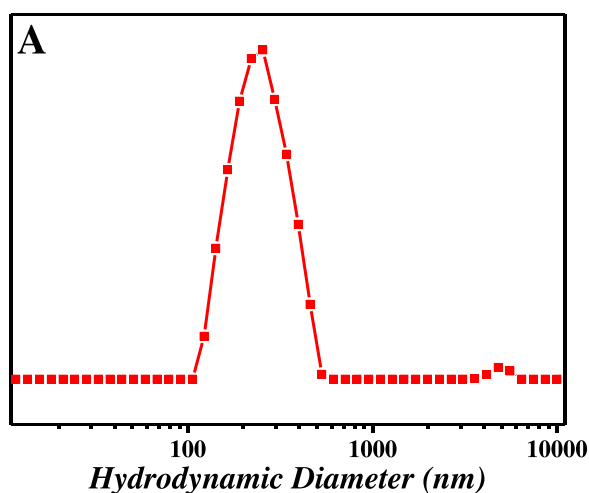
Figure 3. DLS study (A) and SEM image (B) of PNs-Cur.

result in the degradation of the hydrophobic chain of PCL, which has the composition of the hydrophobic core of PNs. After the degradation of PCL, the nanoparticles PNs would disassemble, accompanying the rapid release of embedded curcumin, which would be identified in the absence and presence of lipase by the experiment. As shown in Figure 5, the release of curcumin was very slow from PNs-Cur in the absence of lipase, with about 32.2% being released from PNs-Cur in 60 h. However, after incubation with *Pseudomonas* lipase for 60 h, the release of curcumin quickened and increased significantly. The cumulative release reached 94.6%. Obviously, the results suggested that the bacterial lipase can indeed degrade the PCL core of constructed PNs, simultaneously promoting the release of curcumin.

Antibacterial Activities. The antibacterial activities of PNs-Cur are attributed to loaded curcumin and the protonation of bare amino groups ($-NH_2$) of the PLys block. As shown in Table 1, the MIC data ($12-32$ μg/mL) indicated that PNs-Cur exhibited effective and broad-spectrum antimicrobial activities against both Gram-positive and Gram-negative bacteria, including clinical bacteria *Staphylococcus aureus* (ATCC29213) and drug-resistant bacteria *Pseudomonas aeruginosa*, VRE, and fungus *M. albicans*. Furthermore, the antibacterial activities of PNs-Cur against Gram-positive bacteria are slightly better than that against Gram-negative bacteria, which may be due to the fact that the Gram-negative
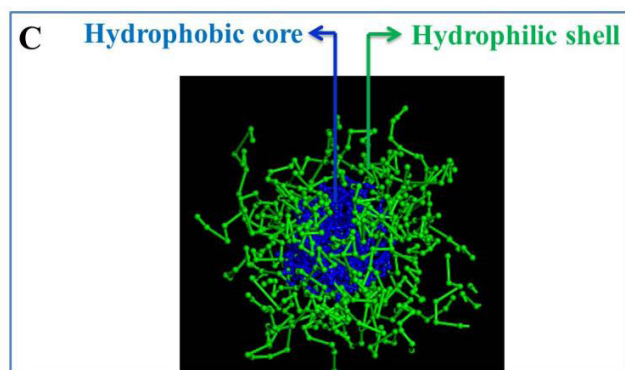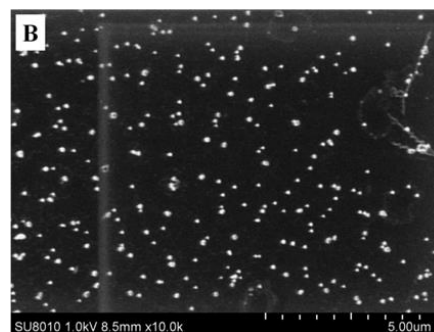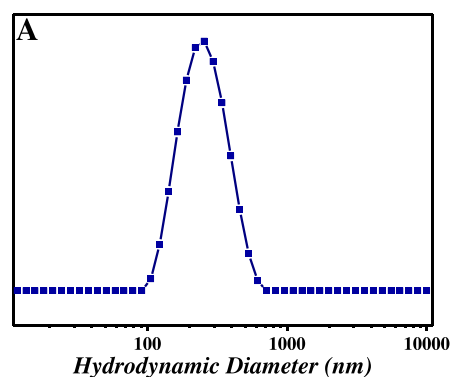
Figure 4. DLS study (A) and SEM image (B) of PNs, and formation of PNs, simulated by molecular modeling using Materials Studio software (C).
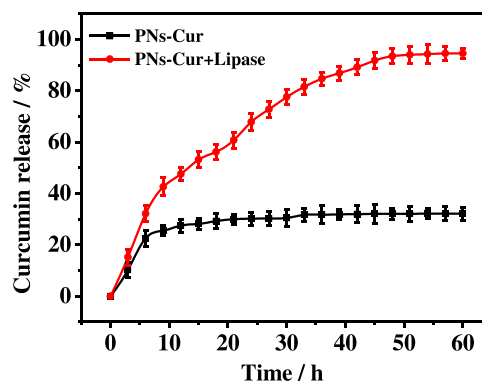
Figure 5. Curcumin release profiles of PNs-Cur in the absence or presence of lipase.

bacteria cells possess a unique protective outer membrane as an armor, which could resist aggression. Furthermore, the sterilization rate of PNs-Cur against the selected bacteria was measured by the colony formation assay as the previously

Table 1. MIC Values and Sterilization Rate of PNs-Cur

	PNs-Cur		PNs
bacterial strains	MIC (μg/mL)	sterilization rate (%)	MIC (μg/mL)
S. aureus (ATCC29213)	16	94.3	26
VRE	16	93.1	26
B. subtilis (ATCC6633)	8	96.8	18
E. faecalis (ATCC29212)	8	95.6	18
E. coli (BL21)	16	91.6	26
P. aeruginosa	32	90.8	42
M. albicans	16	92.5	36

Figure 6. Kinetics of the antimicrobial study of PNs-Cur for *S. aureus* (ATCC29213) (A) and *E. coli* (BL21) (B).

reported method. Importantly, PNs-Cur exhibited a more than 90% antibacterial rate against the tested bacteria, including drug-resistant bacteria.

In addition, we also evaluated the antibacterial activities of PNs, and the results showed that the nanoparticles PNs (unloaded curcumin) exhibit effective antimicrobial activities (MIC: 18−42 μg/mL). Compared with PNs-Cur, PNs displayed weak inhibitory effects on bacterial growth, which is attributed to the fact that curcumin possesses antibacterial activities. The results implied that the antibacterial activities were obviously enhanced when PNs combined with curcumin. In a word, good antibacterial performance exerted by PNs-Cur suggested that there were synergic effects of PNs and curcumin in inhibiting bacteria growth.

Antimicrobial Kinetics. To investigate the time-dependent antibiosis of PNs-Cur at different concentrations against bacteria, Gram-positive *S. aureus* (ATCC29213) and Gram-negative *Escherichia coli* (BL21), as representative strains, were selected for evaluation. The OD$_{600}$ values of the tested bacteria at a certain concentration as a function of time were recorded. As shown in Figure 6, the growth of both bacteria cells was partially inhibited even after 20 h at half-MIC. Clearly, after 10 h, the bacterial growth of both bacteria was significantly inhibited at MIC. Especially, after incubation for 20 h, both tested bacteria cells showed no obvious increase at MIC, suggesting that PNs-Cur did not indeed result in the emergence of drug resistance for bacteria. Notably, PNs-Cur with a concentration ≥ MIC value exhibited effective antibacterial activities. In addition, we counted the number of viable bacteria and evaluated the colony-forming unit (CFU) as a function of time. The number of viable cells was monitored at different time intervals on an agar plate. As shown in Figure S6, the nanocomposite (MIC) took about 300 min to kill 90% of both bacteria. The nanocomposite (2MIC) took about 200 min to kill 90% of bacteria, which suggested that the sterilization rate increased with the increase in the concentration of PNs-Cur and implied that the sterilization speed of PNs-Cur was relatively fast.

Bacterial Resistance Assays. The increasing emergence of bacterial drug resistance has posed a great threat to public health. Therefore, it is necessary to evaluate whether PNs-Cur is possible to accelerate the development of drug resistance. According to the previously reported method,[52] drug-resistant VRE and *P. aeruginosa* exposed to a culture medium with a concentration of sub-MIC were successively fostered for up to 21 passages, recording the updated MIC of each passage. Conventional antibiotics penicillin and ceftriaxone were regarded as positive controls. As shown in Figure 7A,B, the MIC values of penicillin and ceftriaxone increased greatly, and
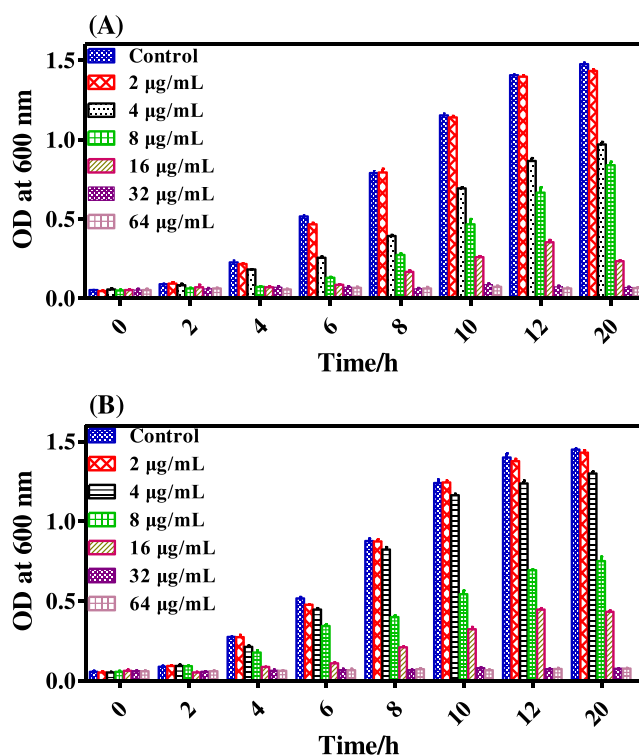
the tested bacteria showed drug resistance only after the 3rd or 4th generation. The MICs of the antibiotics on VRE increased up to 35-fold (Figure 7A) and on *P. aeruginosa* increased up to 30-fold after the 21st passage (Figure 7B). However, the MIC values of PNs-Cur on both bacteria had no dramatic change after the 21st passage, revealing that the nanocomposite did not easily result in drug resistance for the bacteria, which may be due to the fact that PNs-Cur could directly disintegrate the morphology of bacteria. These results suggested that PNs-Cur can be used as a potent antibacterial agent without drug resistance.

Antimicrobial Mechanism. *SEM Analysis.* Generally, the membranes of bacterial cells are negatively charged, while the amino groups (−NH$_2$) of PNs-Cur display positive charges in aqueous solution; therefore, we deemed that the sterilization of PNs-Cur is carried out through the following mode: the nanocomposite with a nanostructure was initially adsorbed onto the surface of bacteria by electrostatic interaction, which can disturb the potential of the membranes and change the selective permeability of the membranes. Meanwhile, the PCL core of PNs-Cur would be degraded and the encapsulated curcumin would be released quickly, further showing antibacterial effects. To verify this mechanism, *S. aureus* (ATCC29213) and *E. coli* (BL21) were chosen for the test. The morphologies of bacteria cells in the presence and absence of PNs-Cur (2MICs) were observed by SEM. As shown in Figure 8A,B, *S. aureus* (ATCC29213) and *E. coli* (BL21) in the absence of PNs-Cur had intact and smooth surfaces, the morphologies of which were regular. However, after incubation with the nanocomposite, the morphologies of both bacteria had mostly been destroyed and collapsed, accompanying the debris of lysing cells. The results suggested that the nanocomposite PNs-Cur could efficiently disorganize and destruct the cell membranes (Figure 8C,D). Especially, this
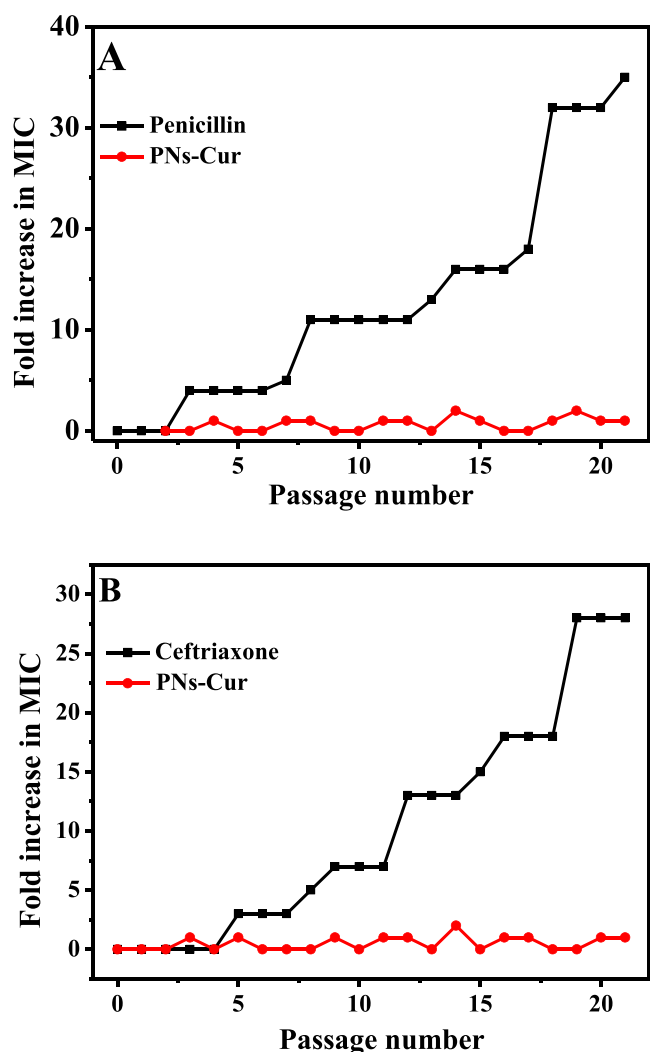
Figure 7. Drug resistance study of PNs-Cur for VRE (A) and *P. aeruginosa* (B).

destructive sterilization mechanism makes the bacteria cells have no opportunity to develop into drug-resistant bacteria.

Fluorescence Staining Experiment. Generally, DAPI could stain bacterial cells, regardless of the activities of the bacteria. However, PI could only stain certain cells of membranes that were damaged. To further demonstrate the rupture of the cell membranes posed by PNs-Cur, fluorescence staining experiments were performed. *S. aureus* (ATCC29213) and *E. coli* (BL21) were stained by DAPI or PI before and after treatment with PNs-Cur. As shown in Figure 9, both bacteria cells stained
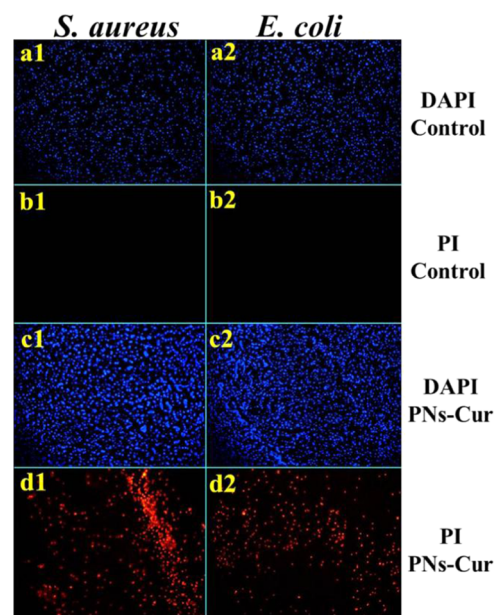

Figure 9. Fluorescence micrographs of (a1−d1) *S. aureus* (ATCC29213) and (a2−d2) *E. coli* (BL21).

by DAPI in the absence of PNs-Cur showed blue fluorescence (Figure 9a1,a2), while both bacteria treated with PI did not produce fluorescence (Figure 9b1,b2), indicating that the
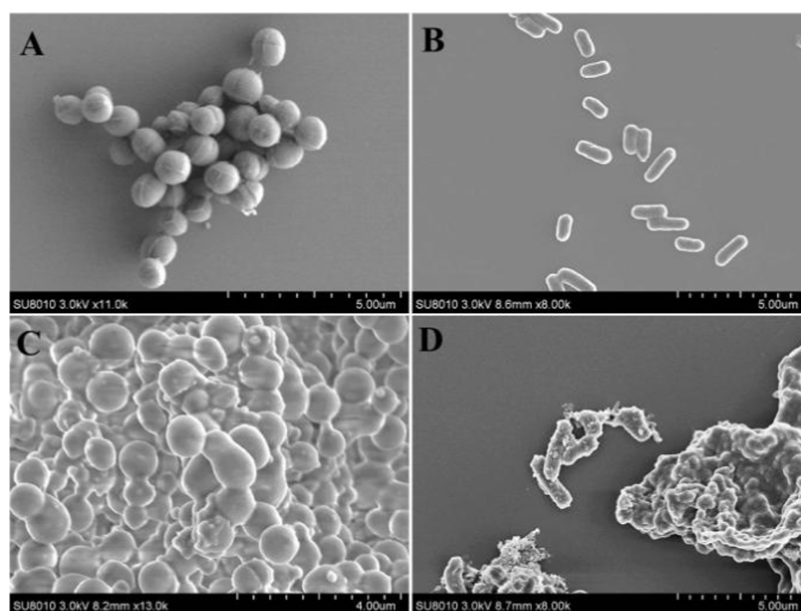

Figure 8. SEM images of *S. aureus* (A−C) and *E.coli* (B−D) before and after treatment with PNs-Cur.

membranes of the chosen bacterial cells were perfect. However, both bacteria cells stained by DAPI or PI in the presence of PNs-Cur produced blue fluorescence and strong red fluorescence, respectively (Figure 9c1,c2,d1,d2), suggesting that the membrane structure of bacteria has been ruptured. These results were consistent with those of SEM, confirming that the nanocomposite could indeed disrupt the cell membranes of bacteria.

Moreover, to evaluate the time-dependent sterilization of PNs-Cur, the fluorescence intensity of the bacterial cells stained with PI in the presence of the nanocomposite was observed. As shown in Figure 10, after incubating with PNs-
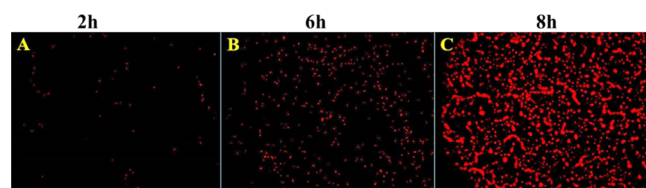

Figure 10. Fluorescence micrographs of *S. aureus* (ATCC29213) exposed to PNs-Cur with different incubation times.

Cur for 2 h, the bacteria cells displayed faint red fluorescence. With the increase of the treatment time, the treated cells fused together and the fluorescence intensity enhanced, indicating that the destruction degree of membranes increased and more cells underwent apoptosis.

Electrolyte Leakage Study. The integrity of cell membranes could avoid the leakage of the cytoplasm including inorganic salt ions such as Na^+, K^+, Mg^{2+}, and Ca^{2+}, ensuring the normal physiological activities of the cells. To investigate whether the cytoplasm would leak after the damage to cell membranes, we monitored the change in the relative conductivity of the bacterial suspension in the presence of PNs-Cur at different intervals. As shown in Figure 11, the relative electrical conductivity of both tested bacterial suspensions changed obviously and increased rapidly in the presence of PNs-Cur. Clearly, the relative electrical conductivity of *S. aureus* (ATCC29213) increased to approximately 73% in 12 h (Figure 11A), while that of *E. coli* (BL21) increased to 63% (Figure 11B); this may be due to the additional outer membranes of Gram-negative bacteria cells. However, both bacterial suspensions without the treatment of PNs-Cur were constant, suggesting that the cytoplasm did not leak. In short, the results indicate that PNs-Cur possesses the ability to destroy cell membranes and cause electrolyte leakage. The antibacterial mechanism of PNs-Cur is different from that of traditional antibiotics and thus is less likely to result in drug resistance, which was consistent with the SEM images and proved that the damage to the bacterial membrane was fast and thoroughgoing.

Surface Plasmon Resonance (SPR) Analysis. To estimate the degree of nanocomposite PNs-Cur-binding bacteria, the experiment surface plasmon resonance (SPR) assay was implemented as previously reported. As a control, the traditional commercial antibiotic faropenem was selected. Briefly, the tested bacteria cells (μRIU = 1000) were immobilized on the chip surface. Then, the PNs-Cur solution with a concentration of 10 mg/mL was injected and passed through the immobilized cells. As shown in Figure 12, the signal values of μRIU increased, indicating that PNs-Cur began to bind to the bacteria cells. Subsequently, the immobilized
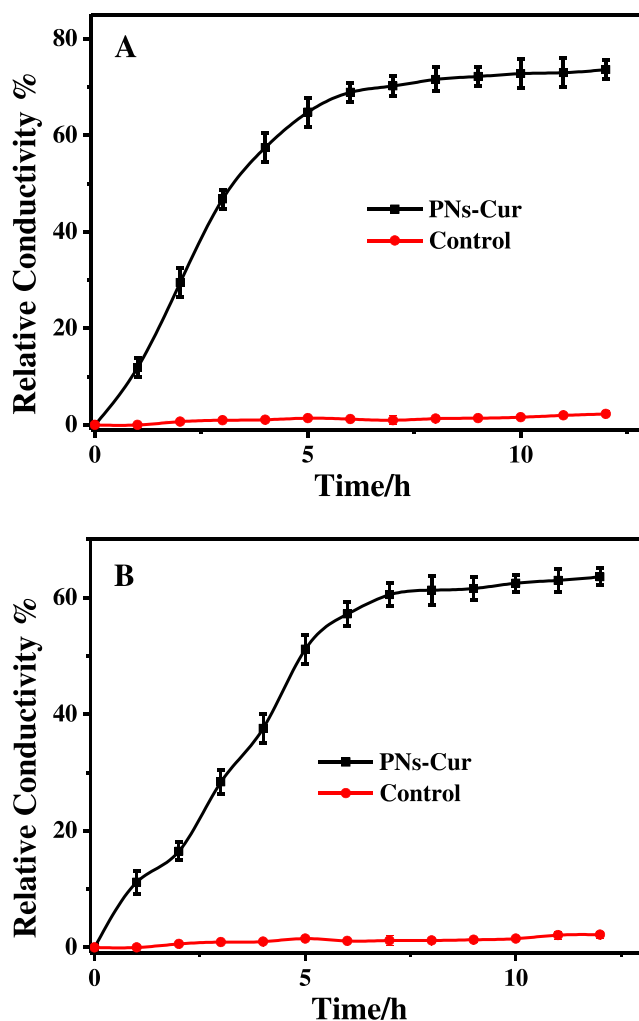

Figure 11. Change in the relative conductivity of *S. aureus* (ATCC29213) (A) and *E. coli* (BL21) (B) suspensions at different intervals.

cells layer on the sensor surface was eluted with buffer, and the signal values of the μRIU of PNs-Cur to both bacteria almost did not decrease, but that of faropenem almost dropped back to the original value, implying that the antibiotic was almost desorbed. The results indicated that the binding affinity of the nanocomposite toward bacteria is stronger than that of faroenem.

Zeta Potential Assay. The nanoparticles PNs-Cur were positively charged, which was attributed to the protonation of the amino groups of PLys chains, which contributed to the more effective interaction between PNs-Cur and bacterial cells. We conducted the cell membrane potential experiments to investigate whether PN-Cur could disturb the membrane potential. *S. aureus* (ATCC29213) and (B) *E. coli* (BL21) were chosen as the Gram-negative and Gram-positive bacteria representatives, respectively. As shown in Table 2, after treatment with PNs-Cur for about 12 h, the membrane potential of both tested bacteria cells increased from −40.6 and −47.8 mV to −3.2 and −9.6 mV (Table 2), respectively. Clearly, the results further confirmed that the nanoparticles PNs-Cur could indeed disturb the balance of the cell membrane potential and show irregular ion movement.

Cytotoxicity Tests. The cytotoxicity of the nanocomposite PNs-Cur with concentrations ranging from 0.002 to 0.52 mg/
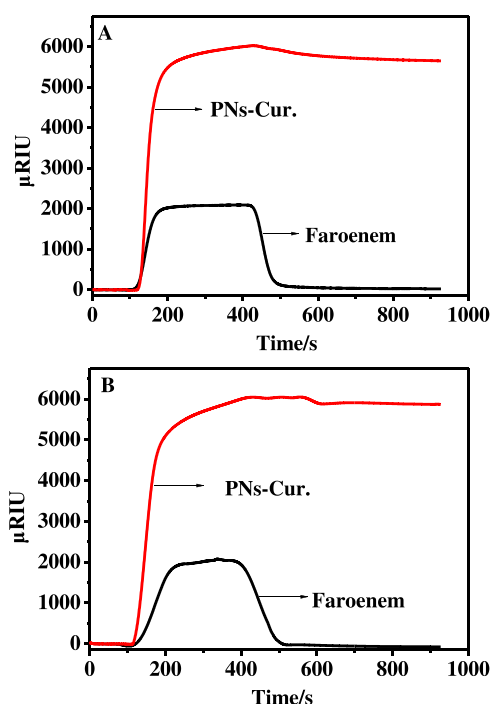
Figure 12. SPR sensorgrams of PNs-Cur and faroenem bind to (A) *S. aureus* (ATCC29213) and (B) *E. coli* (BL21).

Table 2. Zeta Potential (mV) of Bacteria Cell Membranes before and after Treatment with PNs-Cur

	S. aureus (ATCC29213)	*E. coli* (BL21)
control	−40.6 ± 2.3	−47.8 ± 3.6
bacteria/PNs-Cur	−3.2 ± 1.4	−9.6 ± 2.8

mL toward normal mouse fibroblasts (L929) was evaluated by CCK-8. As shown in Figure 13, after treatment with PNs-Cur
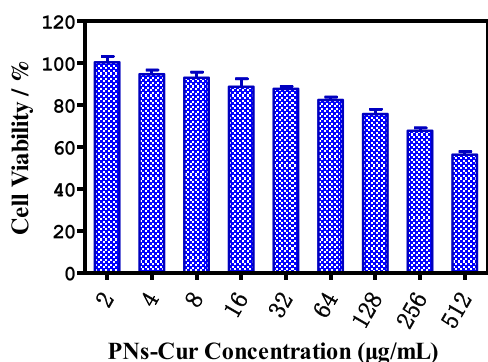

Figure 13. Cytotoxicity study of PNs-Cur against L929 cells at different concentrations.

(concentration ≥128 μg/mL) for 24 h, the viability of cells was maintained at over 80%. This indicated that the nanocomposite possessed the property of low toxicity, which was probably attributed to the good biocompatibility of PCL chains and polypeptide PLys chains and the feature of the nanostructure.

Antibacterial Activity Assay In Vivo. To evaluate the practical antibacterial applicability of PNs-Cur in vivo, we established a mice model by systemic infection by intraperitoneal injection of Gram-negative and Gram-negative

bacteria, in which the parallel mice were randomly divided into three groups, each of six, respectively. MRSA (ATCC43300) (A) and *E. coli* (BL21) (B) were selected for the test. As shown in Figure 14A,B, after treatment with PNs-Cur, the bacterial counts in infected organs (in group 3: heart, liver, spleen, lung, and kidney) significantly decreased. Especially, as shown in Figure 15, all of the mice in group 2 treated with normal saline died after 72 h, and the mice in group 1 as a control injected with the nanocomposite survived. The results suggested that the nanocomposite PNs-Cur not only displayed practical antibacterial activities but also possessed good biocompatibility and low toxicity.

■ CONCLUSIONS

In summary, we designed positively charged nanoparticles PNs by the ring-opening polymerization reaction and then encapsulated natural curcumin into the PCL core of PNs through self-assembly, by which the nanocomposite PNs-Cur were successfully prepared and verified by SEM and DLS assays. Biological assays showed that PNs-Cur possessed great effective sterilization against drug resistance, clinical bacteria, and fungus. Especially, it is most noteworthy that the nanocomposite did not indeed exacerbate the emergence of drug resistance even after the 21st passage. Sterilization mechanism investigation showed that PNs-Cur employed combined modes to kill bacterial cells, including membrane potential destruction, membrane permeability change, DNA damage, enzyme (SDH) synthesis inhibition, and so on, which is attributed to the physicochemical properties of its nanostructure and positively charged surface, ultimately leading to bacteria apoptosis irreversibly. Most importantly, the nanocomposite showed low toxicity regardless of in vivo or in vitro and possessed practically effective antibacterial activities. Overall, this work provides a promising strategy to construct great potential antibacterial materials for nano-biomedical applications.

■ EXPERIMENTAL SECTION

Materials and Characterization. ε-Benzyloxycarbonyl-L-lysine (Lys-Cbz), triphosgene, and ε-caprolactone were purchased from Shanghai Hanhong Chemical Co., Ltd. N-Boc-ethanolamine, hydrogen bromide (30% in acetic acid), trifluoroacetic acid (TFA), tetrahydrofuran (THF), and dimethyl sulfoxide (DMSO) were purchased from Macklin Co., Ltd. Propidium iodide (PI) and diamidino-phenyl-indole (DAPI) were purchased from Sigma-Aldrich (Milwaukee). Pentane, diethyl ether, 2-methylallylamine, dialysis tubing, 2,2-azobisisobutyronitrile, and N,N-dimethylformamide (DMF) were purchased from Aladdin Industrial Corporation. DMF, THF, ε-caprolactone, and the other organic solvents were dried and distilled with calcium hydride or sodium before use. The tested Gram-positive and Gram-negative bacteria were obtained from the Medical College of Xi'an Jiaotong University (Xi'an, China), China. The other reagents were obtained from Sigma-Aldrich Co., Ltd. Normal mouse fibroblast cells (L929) were purchased from the First Affiliated Hospital of Xi'an Jiaotong University. Mice were purchased from the Medical College of Xi'an Jiaotong University.

^{1}H NMR spectra were recorded on a Bruker AV 400 MHz spectrometer, using tetramethylsilane as an internal standard and DMSO-d_6, CDCl$_3$, or D$_2$O as the solvent. UV−vis absorption spectra were recorded on an Agilent UV8453 UV−
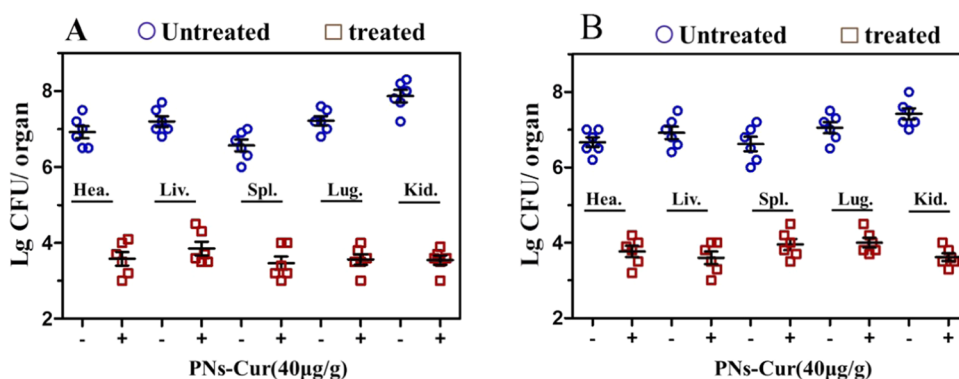
Figure 14. Effect of PNs-Cur on the bacterial counts (MRSA(ATCC29213) (A) and *E. coli* (BL21) (B)) in different organs.
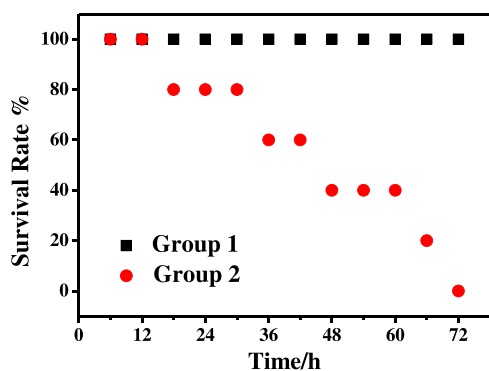

Figure 15. Survival rates of mice in groups 1 and 2.

vis spectrometer. Dynamic light scattering (DLS) and ζ potential experiments were carried out on a Malvern Zetasizer Nano-ZS at a fixed scattering angle of 90°. The morphologies of nanoparticles and bacteria cells were observed utilizing a scanning electronic microscope (NOVA450 SEM, FEI, Eindhoven, The Netherlands), and the test bacterial cells were prepared by spraying a dispersion of bacteria onto a Si slice. Fluorescence spectra were recorded on an FLS 980 spectrofluorometer (Edinburgh Instruments, U.K.) at room temperature. The adsorption and desorption processes between the nanoparticles and cells were monitored by a Reichert SR7500DC dual-channel SPR system.

Synthesis of a Lys-Cbz-NCA Monomer. According to our previous study,[12] dried Lys-Cbz (0.01 mol) was added to anhydrous THF (30 mL) and heated to 50 °C in a round-bottom flask, from which the air was removed by blowing N_2 as much as possible. Then, triphosgene (2.08 g) dissolved in about 10 mL of anhydrous THF was added to the Lys-Cbz suspension under the protection of nitrogen, which was stirred at 50 °C in a N_2 atmosphere for 3 h and then cooled to room temperature. The concentrated mixture was precipitated with excess anhydrous pentane. The achieved white solid was purified by recrystallization with THF/pentane (1:5) and freeze-dried to give the monomer Lys-Cbz-NCA. Yield: ~86%.

Synthesis of Liner PCL-NH-Boc. First, distilled and dried ε-caprolactone (ε-CL, 20.0 mmol) was dissolved in anhydrous toluene ($[\varepsilon\text{-CL}]_0 = 0.9$ M), in which the air was exhausted and filled with nitrogen for about 1 h. Then, the initiator *N*-Boc-ethanolamine (1.0 mmol) and the catalyst methanesulfonic acid (1.0 mmol) were added to the reaction solution, which was stirred at 30 °C for 3 h under nitrogen. Subsequently, Amberlyst A21 was added to the mixture to eliminate the acid

catalyst and then was concentrated under vacuum. The product was then diluted with an appropriate amount of dichloromethane and precipitated in excess methanol. The precipitate was filtered and freeze-dried to offer PCL-NH-Boc. Yield: ~78%.

Synthesis of Liner PCL-NH₂. A PCL-NH$_2$ macroinitiator was prepared through the deprotection of the Boc group of PCL-NH-Boc. First, PCL-NH-Boc (5.0 mg) was fully dissolved into dichloromethane (10 mL), and then trifluoro-acetic acid was added to the mixed solution. After stirring for 5 h at room temperature, the mixture was diluted with an appropriate amount of DMF, which was subsequently precipitated with excess 3−5% $NaHCO_3$ aqueous solution to remove the traces of residual TFA. Finally, a white solid was obtained after freeze-drying. Yield: ~76%. The ^{1}H NMR spectrum of PCL-NH$_2$ is shown in Figure S1 in the Supporting Information.

Synthesis of the Polymer PCL-b-Lys-Cbz. The Lys-Cbz-NCA monomer (20.0 mmol) was fully dissolved in anhydrous DMF (40.0 mL) in a round-bottom flask with a magnetic flea, and then the prepared PCL-NH$_2$ (1.0 mmol) was added to the reaction solution. After stirring for 36 h at room temperature, the reaction solution was concentrated by distillation under reduced pressure and precipitated with excess deionized water. Finally, the product as the precipitant was isolated and freeze-dried to gain the polymer PCL-*b*-Lys-Cbz. Yield: ~72%. The ^{1}H NMR spectrum of PCL-*b*-Lys-Cbz is shown in Figure S2 in the Supporting Information.

Synthesis of the Linear Amphiphilic Polymer PCL-b-Lys. The appropriate amount of PCL-*b*-Lys-Cbz was fully dissolved into TFA in a round-bottom flask with a magnetic flea. Then, excess HBr (30% in acetic acid) was added and stirred at room temperature for 5 h. Subsequently, the target amphiphilic polymer was obtained as a precipitate by the addition of excess diethyl ether into the mixed solution, multiple washing with diethyl ether, dialysis against a 5% $NaHCO_3$ aqueous solution and deionized water for 72 h, and freeze-drying. Yield: ~74%. The ^{1}H NMR spectrum of the PCL-*b*-Lys is shown in Figure S3 in the Supporting Information.

Self-Assembly of PCL-b-Lys into Polymeric Nanoparticles (PNs). The solution of the amphiphilic polymer PCL-*b*-Lys (10 mg) dissolved in THF (4 mL) was added dropwise into deionized water (6 mL) with a dropping funnel. After constantly whisking for 3 h, the resulting solution was dialyzed against deionized water for 48 h to remove small molecules. In addition, the dialyzed medium was renewed after 8 h intervals.

Preparation of the Nanocomposite (PNs-Cur). Curcumin-loaded polymeric nanoparticles (PNs-Cur) were prepared by self-assembling. Briefly, PCL-*b*-Lys (10.0 mg) and curcumin (5.0 mg) were fully dissolved in DMSO (10.0 mL) together, followed by centrifuging for 10 min at 5000 rpm to remove insoluble particles, and the resulting mixture was added dropwise into deionized water (15.0 mL) by a dropping funnel with stirring. After constantly whisking for 8 h, the nanoparticle solution was dialyzed against deionized water in a dialysis tube (molecular weight cutoff 3000 Da) at 25 °C to remove DMSO and the unloaded curcumin. The dialysis medium was renewed every 0.5 h to prepare the curcumin-loaded nanoparticles (PNs-Cur).

Determination of the Critical Nanoparticle Concentration (CNC). The critical concentration of the nanoparticle (CNC) is regarded as the lowest concentration of macromolecules to form nanoparticles in aqueous solution.[11] Pyrene, as the probe, was dissolved in acetone to monitor the formation of nanostructures. First, the solution of pyrene dissolved in acetone (12.6 μg/mL) was prepared and added to volumetric bottles. After acetone evaporation, amphiphilic polymer PCL-*b*-Lys solutions with different concentrations were separately transferred into volumetric bottles and stirred quickly for 24 h at 25 °C. In this experiment, each solution was scanned through emission wavelengths from 365 to 500 nm. Fluorescence intensities of the solutions were recorded with an excitation wavelength of 334 nm, using a 5 nm slit width for excitation and a 2.5 nm slit width for emission. The intensities of I 372 were selected as vibronic bands, and the intensity values were assessed as a function of the log of the concentration of each sample.

Antibacterial Activity (MIC). *Measurement of MIC.* The minimum inhibitory concentration (MIC) values of PNs-Cur were determined according to the Clinical and Laboratory Standards Institute (CLSI) macrodilution (tube) broth method. Therefore, the antibacterial activities of the nanoparticles was evaluated by determining the MIC values in sterile 96-well plates. *S. aureus* (ATCC29213), VRE, *P. aeruginosa*, *E. coli* (BL21), *Bacillus subtilis* (ATCC6633), *Enterococcus faecalis* (ATCC29212), and *M. albicans* were chosen to test antibacterial effects. Briefly, a single colony of the bacteria was transferred into 5 mL of the Mueller−Hinton (MH) culture medium, after culturing at 37 °C for 8 h, which was diluted to about 10^6 CFU/mL with MH broth. The PNs-Cur solution (0.10 mL) with a predetermined concentration ranging from 0.25 to 256 μg/mL and the diluted bacterial suspension (0.10 mL) were added to the 96-well culture plate together and incubated at 37 °C for 16 h. Each evaluation was repeated at least three times.

Measurement of the Bacteriostatic Rate. The bacteriostatic rate of the nanoparticles PNs-Cur was tested according to our previously reported method.[56] The numbers of colony-forming units (CFU) of bacteria treated with the nanoparticles were recorded and expressed as CFU/mL. In the measurement of MIC carried out above, the mixed suspension (0.01 mL) from the well containing PNs-Cur with a concentration of MIC in 96-well plates was diluted, transferred onto an agar plate, and incubated at 37 °C for 16 h. The percentage of the counts of live bacteria in the treated sample compared to the counts in the control sample without any treatment was evaluated.

Resistance Assay. The MICs of PNs-Cur against VRE and *P. aeruginosa* were determined as our previously described

method.[31,52] The employed bacterial strains derived from the well contained PNs-Cur at sub-MICs in 96-well plates for reculturing the next-generation bacteria solution (5 × 10^6 CFU/mL) to obtain the new MICs of the nanoparticles. Importantly, the bacteria were successively passaged for 21 generations, and each updated MIC was redetermined at least three times. As a control, similar experiments were evaluated using penicillin and ceftriaxone

Antimicrobial Kinetics. To evaluate the bactericidal ability of the nanocomposite PNs-Cur, the antibacterial kinetic experiment was carried out as our previously used method. Briefly, PNs-Cur with gradient concentrations was incubated with *S. aureus* (ATCC29213) cells or *E.coli* (BL21, approximately 5 × 10^6 CFU/mL) at 37 °C. After incubation at certain intervals, the OD_{600} value of each mixed suspension was recorded. Moreover, parallel bacterial solutions without nanoparticle treatment were regarded as control groups.

Antimicrobial Mechanism Studies. *Morphological Analysis of Bacterial Cells.* The morphologies of bacteria cells treated with PNs-Cur were investigated by a scanning electronic microscope (SEM).[7,57] Briefly, the cultured bacterial cells (OD_{600} = 0.4−0.6) were treated with the nanoparticles at 2MIC for 8 h, subsequently centrifuged (8000 rpm, 5 min), and washed with sterile PBS. Then, the resulting cells were fixed with 2.5% (v/v) glutaraldehyde for 3 h and washed again with PBS and distilled water separately. The obtained cells were dehydrated employing graded ethanol series (30, 50, 70, 90, and 100%), and then tertiary butyl alcohol was employed to replace ethanol. Ultimately, the prepared cell suspension was dropped on a silicon wafer, freeze-dried, and sprayed with gold for observation.

Fluorescence Staining Experiment. The fluorescence staining experiment is usually used to identify whether the cell membranes are perfect utilizing DAPI and PI. DAPI, a DNA combining fluorescent dye, can stain cells and emit blue fluorescence regardless of whether the membrane is intact or not. PI, a fluorescent dye, cannot pass through intact membranes but can pass through damaged cell membranes and release red fluorescence by excitation. Thus, DAPI and PI can be utilized to investigate whether the cell membrane treated with PNs-Cur is intact or not.[58,59] Briefly, the chosen bacterial cells at the mid-log growth phase (OD_{600} = 0.4−0.6) were incubated with PNs-Cur (2MIC) for 8 h, and the tested cells were separated from the mixed suspension by centrifugation (8000 rpm, 5 min) and washed with sterile PBS. Ultimately, the obtained cells were mixed with PI (5 μg/mL) at 4 °C for 15 min and then washed with excess PBS in the dark. As a comparison, the staining process of cells with DAPI is the same as that with PI. The bacterial cells without nanoparticle treatment were stained only as a control.

Electrolyte Leakage Study. The cell membrane could maintain the relative stability of the intracellular environment and prevent substances from entering or leaving cells freely. Clearly, the damage to the cell membrane can lead to the leakage of the cytoplasm, causing a change in the electrical conductivity of the bacterial suspension.[60,61] Thus, to judge whether the nanoparticles PNs-Cur can destroy the cell membrane, we carried out an experiment of the electrolyte leakage study by measuring the change in the conductivity of the cell suspension as our previously described method. Initially, the chosen strains were cultured to the mid-log growth phase (OD_{600} = 0.4−0.6) at 37 °C, which were collected by centrifugation, washing, and suspending into 5%

glucose, successively. PNs-Cur with a concentration of MIC was added to a 5% glucose solution, and its electric conductivity was recorded to be L_1. Isotonic bacteria suspensions were mixed with the nanoparticles at MIC for 12 h; the electric conductivity of which was marked L_2. In addition, the electric conductivity of isotonic bacteria without any treatment was regarded as a negative control. After ultrasonic crushing, the electric conductivity of isotonic bacteria, as a positive control, was marked L_0. The relative electric conductivity (%) was calculated by the following formula

$$\text{relative electric conductivity}(\%) = \frac{L_2 - L_1}{L_0} \times 100\%$$

Surface Plasmon Resonance (SPR) Analysis. With our previously reported method,[12,52] we monitored the adsorption and elution process of PNs-Cur with bacterial cells by recording the change in the SPR signal. Clearly, the nanoparticles were injected and floated over the cells layer at a precise flow. Then, the cell layer was washed off by a continuous flow of PBS buffer, and the remaining signal reflected the ability of the combination between PNs-Cur and cells. Briefly, the prepared specific bacterial cells (OD_{600}=0.4, 200 μL) were injected and immobilized onto a Au sensor chip. Subsequently, the sensor chip was loaded with PBS buffer for 10 min over two channels to reach equilibrium. While the PNs-Cur solution was fixed onto the immobilized cell surface, the process of binding analysis was carried out. The injection of the PNs-Cur solution lasted for 5 min and the desorption process lasted for 10 min with PBS buffer (10 μL/min), reflecting the changes in the μRIU signal.

Cytotoxicity Assay. Normal mouse fibroblast cells (L929) were chosen to evaluate the cytotoxicity of the nanoparticles PNs-Cur as our previously stated method.[62,63] The cell solution (1.0×10^4 cells/well, 100 μL) was incubated for 24 h in 96-well plates. Subsequently, PNs-Cur with different concentrations was added. To monitor cell viability, the mixture solution (100 μL) composed of medium (99 μL) and DMSO (1 μL) was added to the six wells only containing cells. After incubation for 48 h, the medium was removed. Successively, the fresh culture medium (100 μL) and the cell counting kit-8 solution (10 μL) were mixed together well, incubated for 4 h, and then vigorously shaken. The six wells seeded into the complete medium were regarded as a control. The absorbance at a wavelength of 450 nm was recorded on a microplate reader. All experiments were operated in triplicate.

Antibacterial Activity Assay in Vivo. To evaluate the practical antibacterial activity of PNs-Cur in vivo, we updated a Kunming (SK) male mice infection model as previously reported with slight modification.[52,64] The MRSA (ATCC43300) and *E. coli* (BL21) cells resuspended in sterilized saline were chosen to test. The bacteria-infected KM male mice (20 g/per) were cured with PNs-Cur with a dose of 40 μg/g of the body weight. The healing experiments of MRSA and *E. coli* infection were designed into two parallel experiments, in which the method was the same. Thus, the experiment on MRSA infection and healing mice was regarded as a representative of the following introduction. The mice were randomly divided into three groups, six in each group, in which the two groups were injected with 350.0 μL of the bacterial suspension (1×10^8 CFU/mL), and the third group was not infected. Briefly, uninfected normal group 1, as a control, was used to estimate the cytotoxicity of the nanoparticles PNs-Cur, in which the mice were treated with the PNs-Cur solution every 12 h for 3 days. Similarly, the mice in group 2 were infected with bacteria and then were treated with sterile normal saline every 12 h for 3 days. Especially, the infected mice in group 3 were continuously cured with PNs-Cur every 12 h for 3 days, followed by collection of the same amount of main organs, which were ground in sterilized saline, diluted, and plated on LB agar successively. After culturing at 37 °C for 16 h, the numbers of colony-forming units (CFU) of bacteria cells were recorded by the colony formation assay to evaluate the sterilizing effect. Importantly, the survival rates of mice in groups 1 and 2 were recorded for 3 days.

■ ASSOCIATED CONTENT

Ⓢ Supporting Information

The Supporting Information is available free of charge at https://pubs.acs.org/doi/10.1021/acsomega.2c02855.

■ AUTHOR INFORMATION

Corresponding Authors

Jian Bin Zhen − *Department of Materials Engineering, Taiyuan Institute of Technology, Taiyuan 030008, China;* ⓞ orcid.org/0000-0002-9867-3064; Email: zhenjb187@163.com

Ke-Wu Yang − *Key Laboratory of Synthetic and Natural Functional Molecule Chemistry of Ministry of Education, the Chemical Biology Innovation Laboratory, College of Chemistry and Materials Science, Northwest University, Xi'an 710127, P. R. China;* ⓞ orcid.org/0000-0003-2560-9659; Email: kwyang@nwu.edu.cn

Authors

Jiajia Yi − *School of Materials Science and Engineering, North University of China, Taiyuan 030051, China*

Huan Huan Ding − *Key Laboratory of Synthetic and Natural Functional Molecule Chemistry of Ministry of Education, the Chemical Biology Innovation Laboratory, College of Chemistry and Materials Science, Northwest University, Xi'an 710127, P. R. China*

Complete contact information is available at:
https://pubs.acs.org/10.1021/acsomega.2c02855

Author Contributions

‖J.B.Z. and J.Y. contributed equally to this work.

Notes

The authors declare no competing financial interest.

ACKNOWLEDGMENTS

ABBREVIATIONS USED

NCAs, N-carboxyanhydrides; SEM, scanning electron microscopy; DLS, dynamic light scattering; PNs, polymeric nanoparticles; Cur, curcumin; PCL, polycaprolactone; PLys, polylysine; MIC, minimum inhibitory concentration; CNC, critical nanoparticle concentration; GPC, gel permeation chromatography

REFERENCES

(1) Lima, L. M.; Silva, B.; Barbosa, G.; Barreiro, E. J. β-lactam antibiotics: An overview from a medicinal chemistry perspective. *Eur. J. Med. Chem.* **2020**, *208*, 112829.

(2) Fischbach, M. A.; Walsh, C. T. Biochemistry. Directing biosynthesis. *Science* **2006**, *314*, 603−605.

(3) King, D. T.; Worrall, L. J.; Gruninger, R.; Strynadka, N. C. J. New Delhi Metallo-β-Lactamase: Structural Insights into β-Lactam Recognition and Inhibition. *J. Am. Chem. Soc.* **2012**, *134*, 11362−11365.

(4) Doernberg, S. B.; Lodise, T. P.; Thaden, J. T.; Munita, J. M.; Cosgrove, S. E.; Arias, C. A.; Boucher, H. W.; Ralph, C. G.; Lowy, F. D.; Barbara, M.; Miller, L. G.; Holland, T. L. Gram-Positive Bacterial Infections: Research Priorities, Accomplishments, and Future Directions of the Antibacterial Resistance Leadership Group. *Clinical Infectious Diseases* **2017**, *64*, s24−s29.

(5) Oz, Y.; Ahmed, N.; Stefano, F.; Aarohi, G.; Rui, H.; Amitav, S.; Vincent, M. R. Biodegradable Poly(lactic acid) Stabilized Nanoemulsions for the Treatment of Multidrug-Resistant Bacterial Biofilms. *ACS Appl. Mater. Interfaces* **2021**, *13*, 40325−40331.

(6) Worthington, R. J.; Melander, C. Combination approaches to combat multidrug-resistant bacteria. *Trends Biotechnol.* **2013**, *31*, 177−184.

(7) He, B.; Ma, S.; Peng, G.; He, D. TAT-modified Self-assembled Cationic Peptide Nanoparticles as an Efficient Antibacterial Agent. *Nanomed. Nanotechnol. Biol. Med.* **2018**, *14*, 365−372.

(8) Lam, S. J.; O'Brien-Simpson, N. M.; Pantarat, N.; Sulistio, A.; Wong, E. H.; Chen, Y. Y.; Lenzo, J. C.; Holden, J. A.; Blencowe, A.; Reynolds, E. C.; Qiao, G. G. Combating multidrug-resistant Gram-negative bacteria with structurally nanoengineered antimicrobial peptide polymers. *Nat. Microbiol.* **2016**, *1*, 16162.

(9) Su, Y. J.; Tian, L.; Yu, M.; Gao, Q.; Wang, D. H.; Xi, Y. W.; Yang, P.; Lei, B.; Ma, P. X.; Li, P. Cationic peptidopolysaccharides synthesized by 'click' chemistry with enhanced broad-spectrum antimicrobial activities. *Polym. Chem.* **2017**, *8*, 3788−3800.

(10) Gao, J. Y.; Wang, M. Z.; Wang, F. Y. K.; Du, J. Z. Synthesis and Mechanism Insight of a Peptide-Grafted Hyperbranched Polymer Nanosheet with Weak Positive Charges but Excellent Intrinsically Antibacterial Efficacy. *Biomacromolecules* **2016**, *17*, 2080−2086.

(11) Nederberg, F.; Zhang, Y.; Tan, J.; Xu, K.; Wang, H.; Yang, C.; Gao, S.; Guo, X. D.; Fukushima, K.; Li, L.; et al. Biodegradable nanostructures with selective lysis of microbial membranes. *Nat. Chem.* **2011**, *3*, 409−414.

(12) (a) Zhen, J.-B.; Zhao, M.-H.; Ge, Y.; Liu, Y.; Xu, L.-W.; Chen, C.; Gong, Y.-K.; Yang, K.-W. Construction, mechanism, and antibacterial resistance insight into polypeptide-based Nanoparticles. *Biomater. Sci.* **2019**, *7*, 4142−4152. (b) Konai, M. M.; Jayanta, H. Fatty Acid Comprising Lysine Conjugates: Anti-MRSA Agents That

(13) Hisey, B.; Ragogna, P. J.; Gillies, E. R. Phosphonium-Functionalized Polymer Micelles with Intrinsic Antibacterial Activity. *Biomacromolecules* **2017**, *18*, 914−923.

(14) Mei, L.; Lu, Z.; Zhang, X.; Li, C.; Jia, Y. Polymer-Ag nanocomposites with enhanced antimicrobial activity against bacterial infection. *ACS Appl. Mater. Interfaces* **2014**, *6*, 15813−15821.

(15) (a) Hoque, J.; Konai, M. M.; Samaddar, S.; Gonuguntala, S.; Manjunath, B. G.; Ghosha, C.; Haldar, J. Selective and broad spectrum amphiphilic small molecules to combat bacterial resistance and eradicate biofilms. *Chem. Commun.* **2015**, *51*, 13670−13673. (b) Akash, G.; Ryan, F. L.; Vincent, M. R. Nanoparticle-Based Antimicrobials: Surface Functionality is Critical [version 1; peer review: 2 approved]. *F1000Research* **2016** *5* 364. DOI: 10.12688/f1000research.7595.1.

(16) (a) Deslouches, B.; Montelaro, R. C.; Urish, K. L.; Di, Y. P. Engineered Cationic Antimicrobial Peptides (eCAPs) to Combat Multidrug-Resistant Bacteria. *Pharmaceutics* **2020**, *12*, No. 501. (b) Shu, J. L.; Edgar, H. H. W.; Cyrille, B.; Greg, G. Q. Antimicrobial polymeric nanoparticles. *Prog. Polym. Sci.*, DOI: 10.1016/j.progpolymsci.2017.07.007.

(17) Zhao, R.; Hai, W.; Ji, T.; Anderson, G.; Nie, G.; Zhao, Y. Biodegradable cationic ε-poly-L-lysine-conjugated polymeric nanoparticles as a new effective antibacterial agent. *Science Bulletin* **2015**, *60*, 216−226.

(18) Mortazavian, H.; Foster, L. L.; Bhat, R.; Patel, S.; Kuroda, K. Decoupling the Functional Roles of Cationic and Hydrophobic Groups in the Antimicrobial and Hemolytic Activities of Methacrylate Random Copolymers. *Biomacromolecules* **2018**, *19*, 4370−4378.

(19) Shao, W.; Liu, X.; Min, H.; Dong, G.; Feng, Q.; Zuo, S. Preparation, characterization, and antibacterial activity of silver nanoparticle-decorated graphene oxide nanocomposite. *ACS Appl. Mater. Interfaces* **2015**, *7*, 6966−6973.

(20) Li, Y. M.; Liu, G. H.; Wang, X. R.; Hu, J. M.; Liu, S. Enzyme-Responsive Polymeric Vesicles for Bacterial-Strain-Selective Delivery of Antimicrobial Agents. *Angew. Chem.* **2016**, *128*, 1792−1796.

(21) Plachá, D.; Muñoz-Bonilla, A.; Muoz-Bonilla, A.; Škrlová, K.; Krlová, K.; Echeverria, C.; Chiloeches, A.; Petr, M.; Petr, M.; Lafd, K.; Lafdi, K.; Fernández-García, M. Antibacterial Character of Cationic Polymers Attached to Carbon-Based Nanomaterials. *Nanomaterials* **2020**, *10*, No. 1218.

(22) Miller, K. P.; Wang, L.; Benicewicz, B. C.; Decho, A. W. Inorganic Nanoparticles Engineered to Attack Bacteria. *Chem. Soc. Rev.* **2015**, *44*, 7787−7807.

(23) Thoma, L. M.; Boles, B. R.; Kuroda, K. Cationic Methacrylate Polymers as Topical Antimicrobial Agents against Staphylococcus aureus Nasal Colonization. *Biomacromolecules* **2014**, *15*, 2933−2943.

(24) Sambhy, V.; Peterson, B. R.; Sen, A. Antibacterial and Hemolytic Activities of Pyridinium Polymers as a Function of the Spatial Relationship between the Positive Charge and the Pendant Alkyl Tail. *Angew. Chem., Int. Ed.* **2008**, *47*, 1250−1254.

(25) Ghosh, S.; Haldar, J. Cationic polymer−based antibacterial smart coatings. *Adv. Smart Coat. Thin Films Future Ind. Biomed. Eng. Appl.* **2020**, 557−582.

(26) Guo, W.; Wang, Y. J.; Wan, P. Q.; Wang, H.; Chen, L.; Zhang, S.; Xiao, C.; Chen, X. Cationic amphiphilic dendrons with effective antibacterial performance. *J. Mater. Chem. B* **2022**, *10*, 456−467.

(27) Chen, T.; Zhao, L.; Wang, Z.; Zhao, J.; Yang, M.; et al. Enhancing antibacterial activity of geminized cationic amphiphilic polymer via structure control and self-assembly regulation. *J. Ind. Eng. Chem.* **2020**, *90*, 371−378.

(28) Zhao, S.; Huang, W.; Wang, C.; Wang, Y.; Dong, A.; et al. Screening and Matching Amphiphilic Cationic Polymers for Efficient Antibiosis. *Biomacromolecules* **2020**, *21*, 5269−5281.

(29) Santos, M. R. E.; Mendona, P. V.; Almeida, M. C.; Rita, B.; Serra, A. C.; Morais, P. V.; Coelho, J. F. J. Increasing the Antimicrobial Activity of Amphiphilic Cationic Copolymers by the Facile Synthesis of High Molecular Weight Stars by Supplemental

Activator and Reducing Agent Atom Transfer Radical Polymerization. *Biomacromolecules* **2019**, *20*, 1146−1156.

(30) Wang, X. D.; Yang, F. P.; Yang, H. W.; Zhang, X.; Tang, H. Y.; Luan, S. F. Preparation of antibacterial polypeptides with different topologies and their antibacterial properties. *Biomater. Sci.* **2022**, *10*, 834−845.

(31) Li, Y.; Zhen, J.; Tian, Q.; Shen, C.; Zhang, L.; Yang, K.; Shang, L. One step synthesis of positively charged gold nanoclusters as effective antimicrobial nanoagents against multidrug-resistant bacteria and biofilms - ScienceDirect. *J. Colloid Interface Sci.* **2020**, *569*, 235−243.

(32) Shang, L.; Xu, J.; Nienhaus, G. U. Recent advances in synthesizing metal nanocluster-based nanocomposites for application in sensing, imaging and catalysis. *Nano Today* **2019**, *28*, 100767.

(33) Guo, L. X.; Wang, H. P.; Wang, Y. X.; Liu, F.; Feng, L. H. Organic Polymer Nanoparticles with Primary Ammonium Salt as Potent Antibacterial Nanomaterials. *ACS Appl. Mater. Interfaces* **2020**, *12*, 21254−21262.

(34) Li, Y.; Liu, G. H.; Wang, X. R.; Hu, J. M.; Liu, S. Y. Enzyme-Responsive Polymeric Vesicles for Bacterial-Strain-Selective Delivery of Antimicrobial Agents. *Angew. Chem.* **2016**, *128*, 1792−1796.

(35) Wessels, M. G.; Jayaraman, A. Self-assembly of amphiphilic polymers of varying architectures near attractive surfaces. *Soft Matter.* **2020**, *16*, 623−633.

(36) Yan, J.; Zheng, L. C.; Hu, K.; Li, L. H.; Li, C. C.; Zhu, L.; Wang, H. L.; Xiao, Y. N.; Wu, S. H.; Liu, J. J.; Zhang, B.; Zhang, F. Cationic polyesters with antibacterial properties: Facile and controllable synthesis and antibacterial study. *Eur. Polym. J.* **2019**, *110*, 41−48.

(37) Li, P.; Zhou, C. C.; Rayatpisheh, S.; Ye, K.; Poon, Y. F.; Hammond, P. T.; Duan, H.; Chan-Park, M. B. Cationic Peptidopolysaccharides Show Excellent Broad-Spectrum Antimicrobial Activities and High Selectivity. *Adv. Mater.* **2012**, *24*, 4130−4137.

(38) (a) Chen, J.; Wang, F.; Liu, Q.; Du, J. Antibacterial polymeric nanostructures for biomedical applications. *Chem. Commun.* **2015**, *50*, 14482−14493. (b) Lu, L.; Liang, Y.; Jing, Y.; Chuanbing, T.; Qian, W. Development of Core−Shell Nanostructures by In Situ Assembly of Pyridine-Grafted Diblock Copolymer and Transferrin for Drug Delivery Applications. *Biomacromolecules* **2016**, *17*, 2321−2328.

(39) Gupta, A.; Shazia, M.; Cheng-Hsuan, L.; Irshad, H.; Vincent, M. R. Combatting antibiotic-resistant bacteria using nanomaterials. *Chem. Soc. Rev.* **2019**, *48*, 415−427.

(40) (a) Huh, A. J.; Kwon, Y. J. "Nanoantibiotics": a new paradigm for treating infectious diseases using nanomaterials in the antibiotics resistant era. *J. Controlled Release* **2011**, *156*, 128−145. (b) Makabenta, J. M. V.; Ahmed, N.; Cheng-Hsuan, L.; Schmidt-Malan, S.; Robin, P.; Vincent, M. R. Nanomaterial-based therapeutics for antibiotic-resistant bacterial infections. *Nat. Rev. Microbiol.* **2021**, *19*, 23−36.

(41) Westmeier, D.; Hahlbrock, A.; Reinhardt, C.; Fröhlich-Nowoisky, J.; Wessler, S.; Vallet, C.; Pöschl, U.; Knauer, S. K.; Stauber, R. H. Nanomaterial−microbe cross-talk: physicochemical principles and (patho)biological consequences. *Chem. Soc. Rev.* **2018**, *47*, 5312−5337.

(42) Liu, J.; Sun, Z.; Deng, Y.; Zou, Y.; Li, C.; Guo, X.; Xiong, L.; Gao, Y.; Li, F. Highly Water-Dispersible Biocompatible Magnetite Particles with Low Cytotoxicity Stabilized by Citrate Groups. *Angew. Chem., Int. Ed.* **2009**, *48*, 5875−5879.

(43) Qiao, Y.; Yang, C.; Coady, D. J.; Ong, Z. Y.; Hedrick, J. L.; Yang, Y. Y. Highly dynamic biodegradable micelles capable of lysing Gram-positive and Gram-negative bacterial membrane - ScienceDirect. *Biomaterials* **2012**, *33*, 1146−1153.

(44) Kenawy, E.-R.; Worley, S. D.; Broughton, R. The chemistry and applications of antimicrobial polymers: a state-of-the-art review. *Biomacromolecules* **2007**, *8*, 1359−1384.

(45) Barman, S.; Konai, M. M.; Samaddar, S.; Haldar, J. Amino Acid Conjugated Polymers: Antibacterial Agents Effective against Drug-Resistant Acinetobacter baumannii with No Detectable Resistance. *ACS Appl. Mater. Interfaces* **2019**, *11*, 33559−33572.

(46) Huang, F.; Yang, G.; Zhang, Y.; Cheng, T.; Liu, J.; et al. Silver-Decorated Polymeric Micelles Combined with Curcumin for Enhanced Antibacterial Activity. *ACS Appl. Mater. Interfaces* **2017**, *9*, 16880−16889.

(47) Bhawana Basniwal, R. K.; Buttar, H. S.; Jain, V. K.; Jain, N.; Agric, J. Curcumin Nanoparticles: Preparation, Characterization, and Antimicrobial Study. *Food Chem.* **2011**, *59*, 2056−2061.

(48) Moghadamtousi, S. Z.; Kadir, H. A.; Hassandarvish, P.; Tajik, H.; Abubakar, S.; Zandi, K. A. Review on Antibacterial, Antiviral, and Antifungal Activity of Curcumin. *BioMed Res. Int.* **2014**, *186864*.

(49) Rai, D.; Singh, J. K.; Roy, N.; Panda, D. Curcumin inhibits FtsZ assembly: an attractive mechanism for its antibacterial activity. *Biochem. J.* **2008**, *410*, 147−155.

(50) Anand, P.; Kunnumakkara, A.; Newman, R. A.; Aggarwal, B. B. Bioavailability of curcumin: problems and promises. *Mol. Pharm.* **2007**, *4*, 807−818.

(51) (a) Betts, J. W.; Sharili, A. S.; Ragione, R. M. L.; Wareham, D. W. In Vitro Antibacterial Activity of Curcumin−Polymyxin B Combinations against Multidrug-Resistant Bacteria Associated with Traumatic Wound Infections. *J. Nat. Prod.* **2016**, *79*, 1702−1706. (b) Zhang, J. Y.; Chen, Y. P.; Kristen, P. M.; Mitra, S. G.; Marpe, B.; Yan, Y.; Mitzi, N.; Alan, W. D.; Tang, C. B. Antimicrobial Metallopolymers and Their Bioconjugates with Conventional Antibiotics against Multidrug-Resistant Bacteria. *J. Am. Chem. Soc.* **2014**, *136*, 4873−4876.

(52) (a) Zhen, J. B.; Kang, P. W.; Zhao, M. H.; Yang, K. W. Silver Nanoparticle Conjugated Star PCL-b-AMPs Copolymer as Nanocomposite Exhibits Efficient Antibacterial Properties. *Bioconjugate Chem.* **2020**, *31*, 51−63. (b) Namivandi-Zangeneh, R.; Zahra, S.; Debarun, D.; Mark, W.; Edgar, H. H. W.; Cyrille, B. Synergy between Synthetic Antimicrobial Polymer and Antibiotics: A Promising Platform To Combat Multidrug-Resistant Bacteria. *ACS Infect. Dis.* **2019**, *5*, 1357−1365.

(53) Wang, M.; Zhou, C.; Chen, J.; Xiao, Y.; Du, J. Multifunctional Biocompatible and Biodegradable Folic Acid Conjugated Poly(ε-caprolactone)−Polypeptide Copolymer Vesicles with Excellent Antibacterial Activities. *Bioconjugate Chem.* **2015**, *26*, 725−734.

(54) (a) Dai, X.; Guo, Q.; Zhao, Y.; Zhang, P.; Zhang, T.; Zhang, X.; Li, C. Functional Silver Nanoparticle as a Benign Antimicrobial Agent That Eradicates Antibiotic-Resistant Bacteria and Promotes Wound Healing. *ACS Appl. Mater. Interfaces* **2016**, *8*, 25798−25807. (b) Phuong, P.; Susan, O.; Edgar, H. H. W.; Cyrille, B. Effect of hydrophilic groups on the bioactivity of antimicrobial polymers. Effect of hydrophilic groups on the bioactivity of antimicrobial polymers. *Polym. Chem.* **2021**, *12*, 5689−5703.

(55) Hu, Y.; Zhang, L. Y.; Cao, Y.; Ge, H. X.; Jiang, X. Q.; Yang, C. Z. Degradation behavior of poly(epsilon-caprolactone)-b-poly-(ethylene glycol)-b-poly(epsilon-caprolactone) micelles in aqueous solution. *Biomacromolecules* **2004**, *5*, 1756−1762.

(56) Zhao, M.-H.; Zhen, J.-B.; Yang, K.-W.; Liu, Y.; Li, J.-Q.; Shi, S.-Q.; et al. Quaternized polymer-based nanostructures confer antimicrobial efficacy against multidrug-resistant bacteria. *New J. Chem.* **2020**, *44*, 3874−3881.

(57) Liu, L.; Xu, K.; Wang, H.; Tan, P. J.; Fan, W.; Venkatraman, S. S.; Li, L.; Yang, Y. Y. Self-assembled cationic peptide nanoparticles as an efficient antimicrobial agent. *Nat. Nanotechnol.* **2009**, *4*, 457−463.

(58) Singh, S.; Nimmagadda, A.; Su, M.; Wang, M. H.; Teng, P.; Cai, J. F. Lipidated α/α-AA heterogeneous peptides as antimicrobial agents. *Eur. J. Med. Chem.* **2018**, *155*, 398−405.

(59) Nimmagadda, A.; Liu, X.; Teng, P.; Su, M.; Li, Y.; Qiao, Q.; Khadka, N. K.; Sun, X. T.; Pan, J. J.; Xu, H.; Li, Q.; Cai, J. F. Polycarbonates with Potent and Selective Antimicrobial Activity toward Gram-Positive Bacteria. *Biomacromolecules* **2017**, *18*, 87−95.

(60) Choi, S.; Isaacs, A.; Clements, D.; Liu, D.; Kim, H.; Scott, R. W.; Winkler, J. D.; Degrado, W. F. De novo design and in vivo activity of conformationally restrained antimicrobial arylamide foldamers. *Proc. Natl. Acad. Sci.* **2009**, *106*, 6968−6973.

(61) Liu, R.; Chen, X.; Falk, S. P.; Mowery, B. P.; Karlsson, A. J.; Weisblum, B.; Palecek, S. P.; Masters, K. S.; Gellman, S. H. Structure-

activity relationships among antifungal nylon-3 polymers: identification of materials active against drug-resistant strains of Candida albicans. *J. Am. Chem. Soc.* **2014**, *136*, 4333−4342.

(62) Xi, Y. J.; Song, T.; Tang, S. Y.; Wang, N. S.; Du, J. Z. Preparation and Antibacterial Mechanism Insight of Polypeptide-Based Micelles with Excellent Antibacterial Activities. *Biomacromolecules* **2016**, *17*, 3922−3930.

(63) Ding, H. H.; Chigan, J. Z.; Zhen, J. B.; Liu, L.; Xu, Y. S.; Chen, C.; Yang, K. W. Cholesteroled polymer (Chol-b-Lys)-based nanoparticles (CL-NPs) confer antibacterial efficacy without resistance. *New J. Chem.* **2021**, *45*, 20743−20750.

(64) Chen, W. Y.; Chang, H. Y.; Lu, J. K.; Huang, Y. C.; Harroun, S. G.; Tseng, Y. T.; Li, Y. J.; Huang, C.; Chang, H. T. Self-Assembly of Antimicrobial Peptides on Gold Nanodots: Against Multidrug-Resistant Bacteria and Wound-Healing Application. *Adv. Funct. Mater.* **2015**, *25*, 7189−7199.